

Design and Control of Grid Interfaced Voltage Source Inverter with Output LCL Filter

Sajad Sarajian^{*1}

¹Department of Electrical Engineering, Islamic Azad University, Ashtian Branch, Ashtian, Iran

June 8, 2014

Abstract

This paper presents design and analysis of an *LCL*-based voltage source converter using for delivering power of a distributed generation source to power utility and local load. *LCL* filter in output of the converter analytically is designed and its different transfer functions are obtained for assessment on elimination of any probable parallel resonant in power system. The power converter uses a controller system to work on two modes of operation, stand-alone and grid-connected modes, and also has a seamless transfer between these two modes of operation. Furthermore, a fast semiconductor-based protection system is designed for the power converter. Performance of the designed grid interface converter is evaluated by using an $85kVA$ industrial setup.

Keywords : Voltage source inverter, grid-interfaced converter, filters Design, power electronics, digital controller.

1 Introduction

Distributed Generation (DG) systems such as microturbines, fuel cells, wind turbines and photovoltaic systems are expected to represent a large portion of power generation capacity, especially in future [1]. In particular, Micro Turbine Generator (MTG) is witnessed to be capable of delivering clean energy from a wide variety of fuels with superior safety and low emissions [2, 3]. The capacity of MTG can be ranged from several kilowatts up to megawatts. As it is often sited dispersedly near the industrial load, it is deemed as a category of distributed generations nowadays [4, 5]. A direct merit exhibited by such electric power generation is to provide the utility a way to defer power plant construction, while offering customers a clean resource at reasonable cost.

^{*}sajadsarajian@yahoo.com

There are essentially two types of micro turbine designs. One is a split shaft design that uses a power turbine rotating at $3600rpm$ and a conventional generator (usually induction generator) connected via a gearbox. The power inverters are not needed in this design. Another is a high-speed single-shaft design with the compressor and turbine mounted on the same shaft as the Permanent Magnet (PM) synchronous generator.

The advantages of the high-speed permanent-magnet generator are its compact size, low-mass design and the elimination of the gearbox, resulting in reduction and simplification of the generating package. The use of power electronics enhances the system performance because of the asynchronous operation of the gas turbine, with the gas turbine speed independent of the grid frequency. It enables the gas turbine speed control to adjust for optimal gas turbine efficiency [6, 7].

A general view of microturbine system is shown in Figure 1. The configuration of an MTG system is composed of a gas turbine, a compressor, and an AC generator. They are inertia welded on a single shaft to simplify the mechanical structure. When this shaft turns at the speed of the turbine, the generator would provide high-frequency AC electricity that requires a rectifier (Converter 1 in Figure 1) and an inverter (Converter 2 in Figure 1) to interface with utility network. By employing different control strategies, the MTG can operate as a power conditioner for the grid-connected operation to improve the quality of supplying power or sever from the grid as an emergency generator [8, 9]. The grid-connected inverter in MT's power electronic interface should operate in grid-tied and

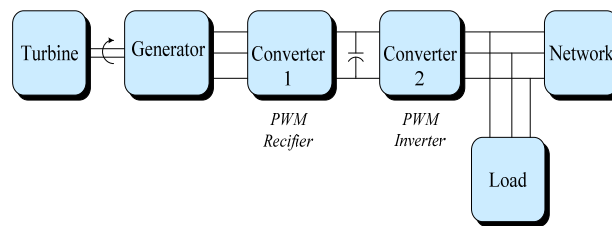


Figure 1: Block diagram of power electronic interface configuration for a MT.

off-grid modes in order to provide power to the emergency load during system outages. Moreover, the transition between the two modes should be seamless to minimize any sudden voltage change across the emergency load or any sudden current change to the grid. A seamless transfer between both modes has been proposed in [10–12]. However, the grid current controller and the output voltage controller must be switched between the two modes, so the outputs of both controllers may not be equal during the transfer instant, which will cause the current or voltage spikes during the switching process. On the other hand, as the grid-interactive inverter should operate in off-grid mode, the filter capacitor is necessary. Nevertheless, the filter capacitor current affects the waveform quality of the grid current in polluted grid, especially at low output power [13–16].

This paper deals with design and construction of a three-phase $85kVA$ grid-interactive inverter and its Digital Signal Processor (DSP)-based digital controller. Two different control modes are considered for the inverter: stand-alone control mode, and grid-connected control mode. Furthermore the inverter controller is expected to have a soft and seamless transfer between these

two control modes. In the following sections, first the overall configuration of system is discussed in section 2, and then in section 3, the controller of inverter is described; in section 4 design procedure for digital controller are explained. Section 5 shows the experimental results of the implemented inverter; paper's conclusion is also presented in section 6.

2 Three-Phase Grid Interactive Inverter

Power configuration of the developed system is depicted in Figure 2. It consists of a primary power source, a full bridge diode rectifier, a DC-link, a full bridge grid converter with LC filter, a power electromechanical relay K , and the three-phase 400V/50Hz grid. The primary power source is, in fact, a microturbine generator that in this study is replaced with a grid connected power autotransformer. The parameters used in the constructed system are shown in Table 1.

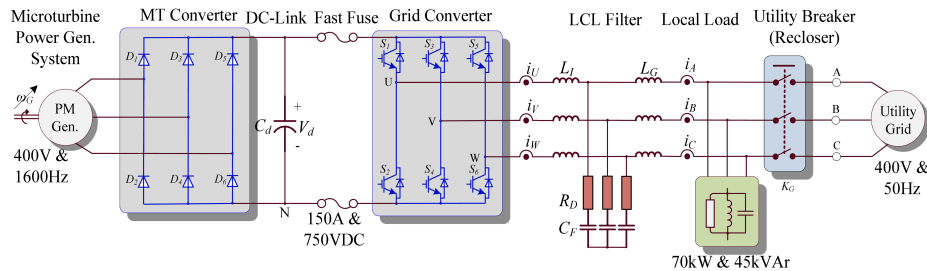


Figure 2: General configuration of constructed grid-tied inverter.

3 Digital Controller of Inverter

A control technique should be designed for inverter (750V_{dc}/400V_{ac}(L-L), rated 70kW) to satisfy following performance characteristics:

1. Low load regulation (less than 5%): the AC output voltage of the DG system should be maintained at 400V (L-L)/230V (L-N) independent of load conditions,
2. Minimum Total Harmonic Distortion (THD): DG system when feeding to the nonlinear loads, such as rectifiers, Switched Mode Power Supplies (SMPS), must generate minimum harmonics currents and voltages in compliant with IEEE 519 std,
3. Fast transient response: system must be able to produce output AC voltage with minimum overshoot or undershoot,
4. Short circuit protection: system must be able to provide protection from excessive overload conditions,

Table 1: System Parameters

Parameter	Value
System voltage: $V_{L-L}(= Vb)$	$400V_{rms}$
Fundamental frequency: f_{Line}	$50Hz$
Load rated: $P_n, Q_n, S_n(= Sb)$	$70kW, 45kVAr, 85kVA$
DC link voltage: V_{dc}	$760V_{dc}(1.9p.u.)$
DC-link Capacitor: C_{dc}	$4200\mu F$
Switching Frequency	$2kHz(40p.u.)$
Sampling Frequency	$4kHz(80p.u.)$
PI controller	$K_p = 0.5, K_I = 200$
Load Power Factor	0.85
System impedance parameters: L_S, R_S	$55\mu H, 2.5m\Omega$
<i>LCL</i> filter parameters:	
L_1, R_1	$0.83mH(13.85\%), 52m\Omega$
L_2, R_2	$0.75mH(12.52\%), 12m\Omega$
C_F	$270\mu F(15.97\%)$
R_d	$0.6\Omega(31.88\%)$
f_{res}	$488Hz(976\%)$

5. Different control modes: the microturbine grid converter should operate in both grid-connected control mode and stand-alone control mode,
6. A soft and seamless transfer between different control modes: in transition from one control mode to the other, amplitude and frequency of the voltage at the PCC must not exit its limitation ($V_{rated} \pm 10\% \& f \pm 2Hz$),
7. Anti-islanding detection capability: based on IEEE 1547 std [17], all DGs must be disconnected from an islanded grid in a specified time,
8. Paralleling capability: in order to increase the reliability of power source converter, it should operate in parallel with other converters, especially in stand-alone operation mode,
9. Deals with distorted and/or unbalanced grid voltage: grid voltage is commonly distorted and/or unbalanced. Therefore, it causes grid-tied inverters to inject a distorted and/or unbalanced current to the power system. So, inverter's controller must be able to suppress these harmonic effects.
10. Decoupled P & Q control for grid-connected inverter: in grid-connected control mode the control of the active and reactive power must be decoupled from each other.

voltage reference in the allowed range, and for fast response there is a direct forward connection to the voltage controller output. This situation can occur if at a certain load, the generated power decreases due to lower microturbine input fuel or during overloading.

3.2 Grid-Tied Mode Operation

In grid-connected control mode, principally all the available power that can be obtained from the microturbine is delivered to the grid. Moreover, compensation of reactive power is possible if required. The block diagram of control arrangement for grid-connected control mode is demonstrated in Figure 4. Standard PI controllers are used to adjust the grid currents in the dq-synchronous frame.

A decoupling of the cross-coupling is implemented in order to compensate the couplings due to the output filter [20, 21]. In order to achieve a zero phase angle between voltage and current, the reference current in the q-axis, I_q^* , of the current loop is in general set to zero and so unity power factor can be achieved.

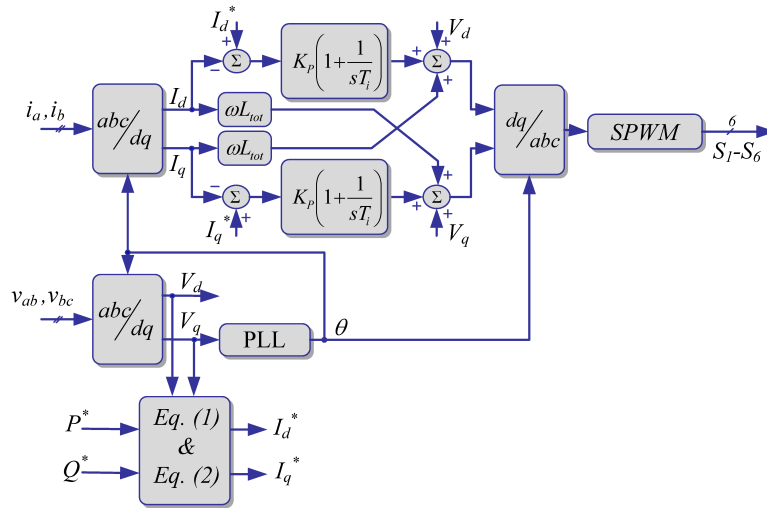


Figure 4: Block diagram of grid-connected inverter control mode.

In grid connected control mode, the controller works as current controller. It sets the voltage reference for a standard Sinusoidal Pulse Width Modulation (SPWM) that generates pulses for the switches of the grid converter via a shielded cable link. A Phase Locked Loop (PLL) is designed to make the inverter synchronism with grid. Also, the reference currents in d_q -axis, I_d^* and I_q^* , can be

drawn from the following relations:

$$p = v_d i_d + v_q i_q \xrightarrow{v_q=0} i_d^* = \frac{p^*}{v_d} \quad (1)$$

$$q = v_d i_q - v_q i_d \xrightarrow{v_q=0} i_q^* = \frac{q^*}{v_d} \quad (2)$$

where v_d and v_q are the grid voltage in d_q -axis, and p^* and q^* are reference active and reactive power that inverter is expected to deliver to the grid.

Furthermore, current feedback PI control with grid voltage feed-forward is commonly used in stationary reference frame for current-controlled inverters. But these solutions have two main drawbacks: inability of the PI controller to track a sinusoidal reference without steady-state error and poor disturbance rejection capability. This is due to the definite control loop gain required for system stability at the *LCL*-filter resonance frequency. Grid voltage feed-forward is often used to get a good dynamic response, but this leads in turn to the increase of the grid-voltage background harmonics in the current waveform because of the imperfect compensations [22].

3.3 Seamless Transfer

In order to realize the seamless transfer between grid-tied and off-grid modes, the load voltage must match the magnitude, frequency, and phase of the grid voltage well before connecting to the utility. The load voltage can match the grid voltage well through sampling the grid voltage as the reference voltage before connecting to the grid, especially in polluted grid voltage. The detailed process of the seamless transfer between the two modes is illustrated in the following.

1. Off-grid mode to grid-tied mode:

- Detect that the grid is normally operating.
- Adjust the inverter's output voltage (or load voltage) to match the magnitude and phase of the grid voltage.
- Once the load voltage is equal to the grid voltage, turn on the relay K and switch inverter from voltage-controlled mode to current-controlled mode, with the reference current being equal to the load current.
- Change the reference current slowly to the desired current (both magnitude and phase).

2. Grid-tied mode to off-grid mode:

- Detect a fault on the grid and give a turn off signal to the relay K .
- Monitor the magnitude and phase of the load voltage.
- When the relay current goes to zero, transit the inverter to a voltage-controlled mode, with the voltage reference being derived from the load voltage.
- Ramp up the magnitude of the load voltage from its initial value to the rated value.

4 Controller Design

Power electronic interface should be operated in standalone and grid connected mode. System model with designed parameters are used to design the system controller. Here, control approach at both operation modes is done.

4.1 Current Controller Design at Grid Connected Mode

Figure 5 shows the single phase equivalent circuit of the grid connected inverter to design linear controller; switch S status determines whether system is operated at off grid mode or grid tied mode. Where LCL parameters are as: $L_I = 0.9mH$, $L_G = 1mH$, $C_f = 84\mu F$, $R_d = 2.1\Omega$ and $Z_L = 8$.

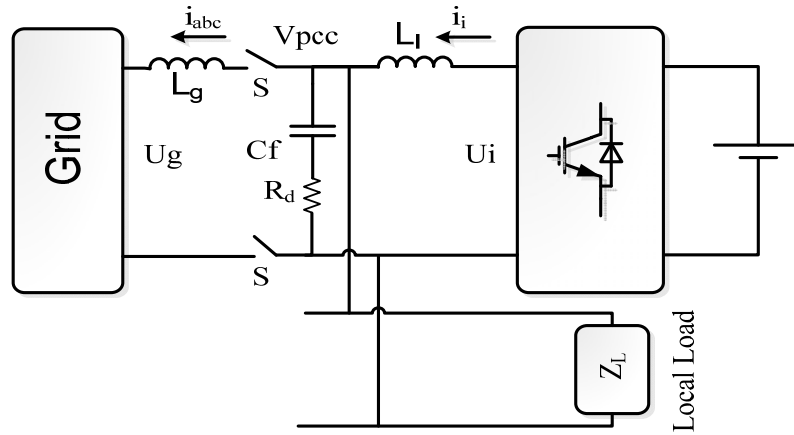


Figure 5: Single phase equivalent circuit of the grid connected inverter.

Controller circuit is designed to control inverter at grid connected and stand alone modes. The standard PI controller with feedback control mode is used; as shown in Figure 6, U_g (grid voltage feed-forward) is an input disturbance. Control method aims to produce the suitable inverter output voltage so that inverter output current is regulated. As a result, required active and reactive power is delivered to grid [20].

PI controller is designed as:

$$G_{PI}(S) = K_P + \frac{K_I}{S} \quad (3)$$

The plant transfer function in terms of inverter output voltage and current is defined as [20]:

$$H_f(S) = \frac{i_i(S)}{U_i(S)} = \frac{L_I C_F S^2 + R_D C_F S + 1}{L_I L_G C_F S^3 + (R_D L_I C_F + R_D L_G C_F) S^2 + (L_I + L_G) S} \quad (4)$$

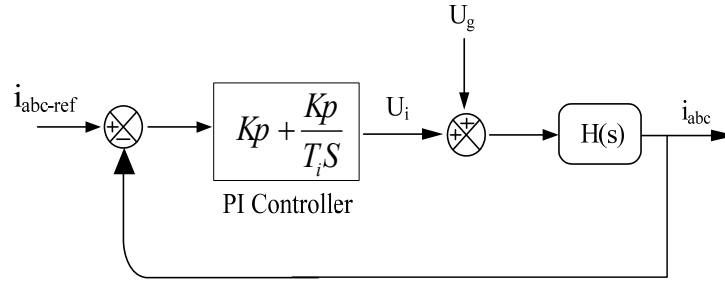


Figure 6: PI controller scheme at grid connected mode.

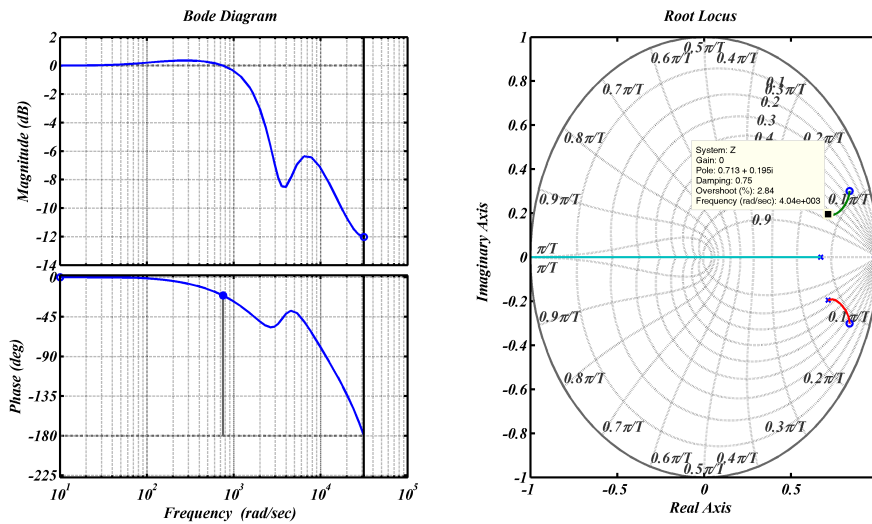


Figure 7: System plots of closed loop system in grid connected mode (a) root-locus map (b) the bode plot.

Figure 7 shows pole-zero plot of open loop system. There are two complex poles and one real pole. Steady state errors and dynamic criteria are used to design integrator gain K . Proportional gain is chosen 4 to achieve damping value $\zeta = 0.7$. The integrator time constant T_i was chosen 9 millisecond as a compromise between noise cancellation and system dynamic.

4.2 Voltage Controller Design in Standalone Mode

The control scheme is shown in Figure 8. Inverter output voltage is used in closed loop system.

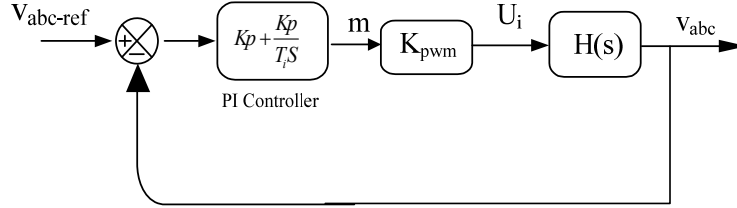


Figure 8: Control scheme in stand-alone mode.

Where plant transfer function $H(S)$ is defined in terms of load voltage V_{pcc} and inverter output voltage U_i ; Z_L is the load equivalent impedance [20].

$$\begin{aligned}
 H(S) &= \frac{v_{pcc}(S)}{U_i(S)} \\
 &= \frac{R_D Z_G C_F S + Z_G}{L_I L_G C_F S^3 + ((R_D + Z_G) L_I C_F + R_D L_G C_F) S^2 + (L_I + L_G + R_D + Z_G + C_F) S + Z_G} \quad (5)
 \end{aligned}$$

$K_p = 0.08$ and $K_i = 0.0002$ are determined as optimal parameters. Figure 9 (a) and (b) show the zero-pole placement at the open-loop and closed loop system plot. Damping factor is 1 at dominant pole and overshoot is negligible. Closed loop system is stable as well.

5 Experimental Results

The constructed inverter is tested under different load and grid scenarios. A photograph of constructed setup is shown in Figure 10. First, islanding operation of inverter is evaluated. Figure 11 shows the experimental results of this test. In Figures 11(a) and (c) the reference voltage in d -axis, V_{d-ref} , is changed from a positive value to a negative value with a similar amplitude but different sign. It means that the voltage amplitude always remain constant but the voltage phase suddenly changed by a 180° step. Figures 11 (b) and (d) are demonstrated the experimental results of islanding operation when the reference voltage is changed between two different constant values. Experimental results shows the inverter have a good performance in the stand-alone mode of operation.

Second test scenario is the seamless transfer process between two control modes. Figs 12(a) and (c) shows first step of seamless transfer process described in section 3.3.1. In these Figures the bottom waveform is the phase difference between voltages at the PCC and the grid, named $\Delta\theta_{PG}$. Figure 12 (b) demonstrates one step of seamless transfer process. The fourth waveform, CSG, shows a criterion variable that DSP evaluates the seamless transfer before sending a closing command to the relay K . Also, the third waveform shows the feedback signals that relay K send

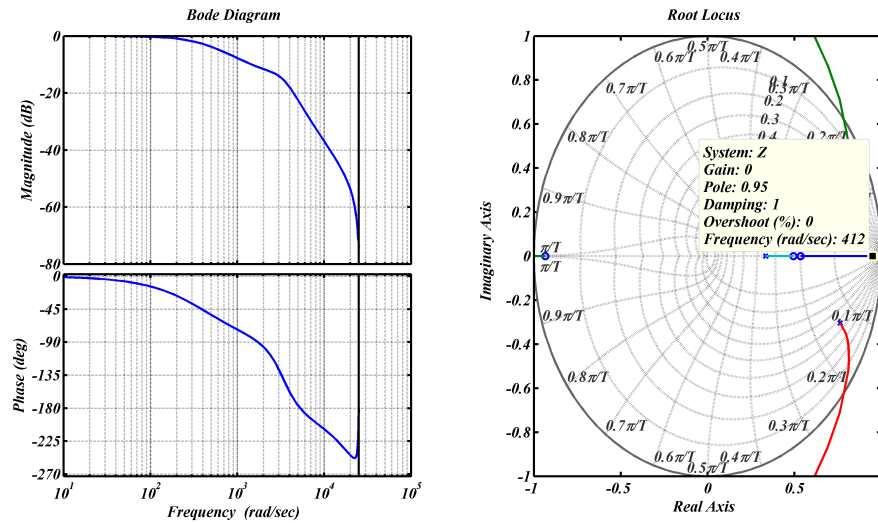


Figure 9: Plots of closed-loop system in stand-alone mode (a) root-locus map (b) the bode plot open-loop.

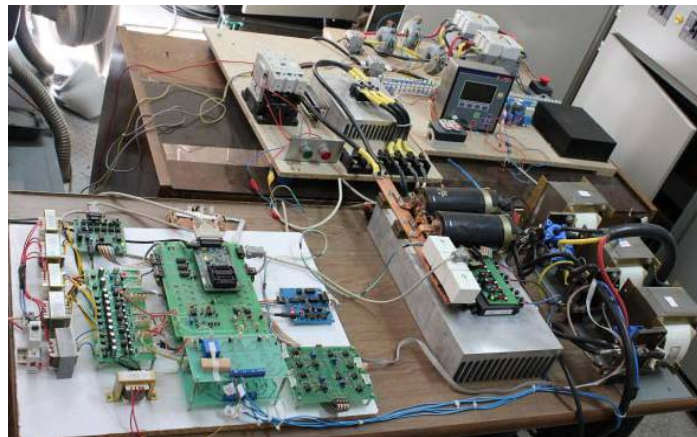


Figure 10: Photograph of constructed DC/AC converter.

back to the DSP and shows the present status of relay. Figure 12 (d) shows the output signal of PLL that is the voltage phase in grid side.

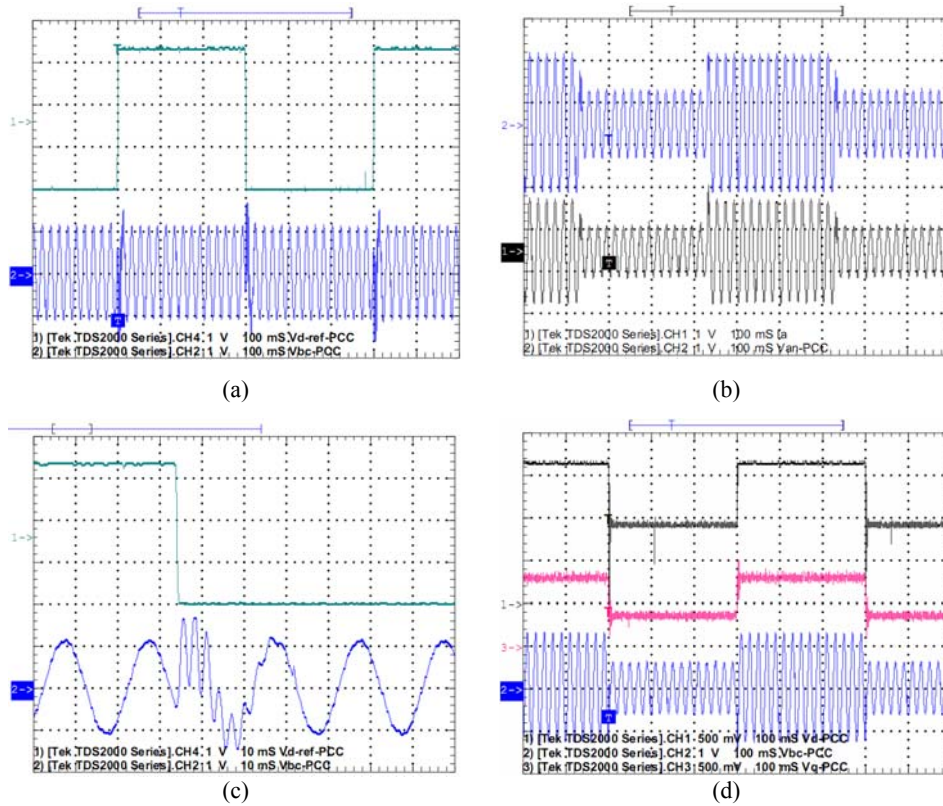


Figure 11: Experimental results when the inverter works in stand-alone mode: waveforms from top to bottom are (a, and c) V_{d-ref} & V_{ab-PCC} ; (b) V_{ab-PCC} & i_a ; (d) V_{d-PCC} & V_{q-PCC} & V_{ab-PCC} .

6 Conclusion

Inverter is an important part of a microturbine-based distribution generation system. In this paper, a DSP-based digital controller in order to control a three-phase inverter in stand-alone and grid-connected modes is studied. The three-phase inverter, in fact, is a three-leg power converter which is switched in $2kHz$ frequency by the controller with a sinusoidal PWM pattern. An $85kVA$ three-phase inverter setup is developed and tested under different source and load scenarios. Experimental results prove the effectiveness and appropriate operation of designed controller. Based on experimental results in stand-alone control mode, output voltages are sinusoidal and balanced only with a low distortion level (voltage THD is less than 3%). In grid-connected control mode, distortion on grid voltage results a distorted inverter output current. To compensate this distortion, a harmonics suppression control block must be added to the inverter controller. The experimental

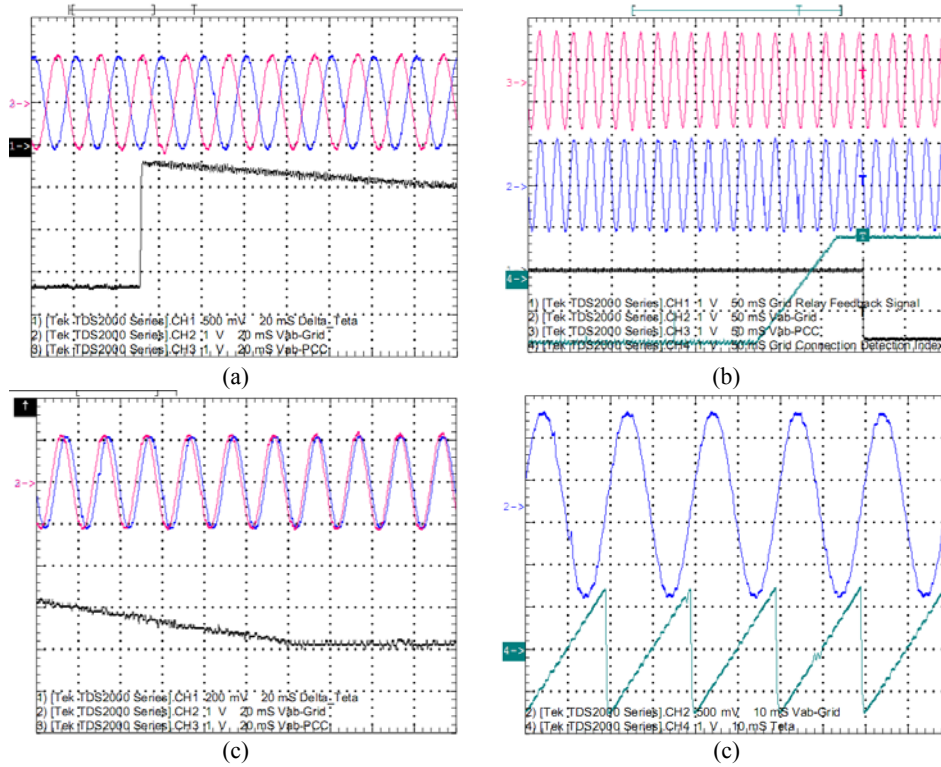


Figure 12: Experimental results when the inverter works in seamless transfer process: waveforms from top to bottom are (a, and c) V_{ab-PCC} , $V_{ab-grid}$ & $\delta\theta_{PG}$; (b) $V_{ab-grid}$ & V_{ab-PCC} & SFR & CSG ; (d) $V_{ab-grid}$ & θ_{PLL} .

results show that seamless transfer between two modes has been achieved well, but because of polluted grid voltage, waveform quality of the grid current is not good.

References

- [1] A. Hasanzadeh, C. Edrington, N. Stroupe, and T. Bevis, "Real-time emulation of a high-speed microturbine permanent-magnet synchronous generator using multiplatform hardware-in-the-loop realization," *Industrial Electronics, IEEE Transactions on*, vol. 61, no. 6, pp. 3109–3118, June 2014.
- [2] H. Karegar and A. Shabani, "Effects of inverter modulation index on the stability of grid

- connected micro-turbines,” in *Power and Energy Conference, 2008. PECTon 2008. IEEE 2nd International*, Dec 2008, pp. 1623–1627.
- [3] Z. Ye, T. Wang, G. Sinha, and R. Zhang, “Efficiency comparison for microturbine power conditioning systems,” in *Power Electronics Specialist Conference, 2003. PESC '03. 2003 IEEE 34th Annual*, vol. 4, June 2003, pp. 1551–1556 vol.4.
- [4] M. S. Laili, Z. N. Zakaria, N. Halim, and P. Ibrahim, “Modelling and simulation of microturbine for a distribution system network with hybrid filter,” in *Power Engineering and Optimization Conference (PEDCO) Melaka, Malaysia, 2012 Ieee International*, June 2012, pp. 204–208.
- [5] L. Wang and G.-Z. Zheng, “Analysis of a microturbine generator system connected to a distribution system through power-electronics converters,” *Sustainable Energy, IEEE Transactions on*, vol. 2, no. 2, pp. 159–166, April 2011.
- [6] M. Ranjbar, S. Mohaghegh, M. Salehifar, H. Ebrahimirad, and A. Ghaleh, “Power electronic interface in a 70 kw microturbine-based distributed generation,” in *Power Electronics, Drive Systems and Technologies Conference (PEDSTC), 2011 2nd*, Feb 2011, pp. 111–116.
- [7] S. Nayak and D. Gaonkar, “Modeling and performance analysis of microturbine generation system in grid connected/islanding mode,” in *Power Electronics, Drives and Energy Systems (PEDES), 2012 IEEE International Conference on*, Dec 2012, pp. 1–6.
- [8] F.-S. Pai and S.-J. Huang, “Design and operation of power converter for microturbine powered distributed generator with capacity expansion capability,” *Energy Conversion, IEEE Transactions on*, vol. 23, no. 1, pp. 110–118, March 2008.
- [9] Y.-R. Mohamed, “Mitigation of dynamic, unbalanced, and harmonic voltage disturbances using grid-connected inverters with lcl filter,” *Industrial Electronics, IEEE Transactions on*, vol. 58, no. 9, pp. 3914–3924, Sept 2011.
- [10] M. Ranjbar, H. Ebrahimirad, S. Mohaghegh, and A. Ghaleh, “Seamless transfer of three-phase grid-interactive microturbine inverter between grid-connected and stand-alone modes,” in *Electrical Engineering (ICEE), 2011 19th Iranian Conference on*, May 2011, pp. 1–1.
- [11] T.-V. Tran, T.-W. Chun, H.-H. Lee, H.-G. Kim, and E.-C. Nho, “Pll-based seamless transfer control between grid- connected and islanding modes in grid-connected inverters,” *Power Electronics, IEEE Transactions on*, vol. PP, no. 99, pp. 1–1, 2013.
- [12] D. Ochs and B. Mirafzal, “A method of seamless transitions between grid-tied and stand-alone modes of operation for utility-interactive three-phase inverters,” *Industry Applications, IEEE Transactions on*, vol. PP, no. 99, pp. 1–1, 2013.
- [13] F. Gonzalez-Espin, G. Garcera, I. Patrao, and E. Figueres, “An adaptive control system for three-phase photovoltaic inverters working in a polluted and variable frequency electric grid,” *Power Electronics, IEEE Transactions on*, vol. 27, no. 10, pp. 4248–4261, Oct 2012.

- [14] M. Castilla, J. Miret, A. Camacho, J. Matas, and L. de Vicuna, "Reduction of current harmonic distortion in three-phase grid-connected photovoltaic inverters via resonant current control," *Industrial Electronics, IEEE Transactions on*, vol. 60, no. 4, pp. 1464–1472, April 2013.
- [15] Z. Liu, J. Liu, and Y. Zhao, "A unified control strategy for three-phase inverter in distributed generation," *Power Electronics, IEEE Transactions on*, vol. 29, no. 3, pp. 1176–1191, March 2014.
- [16] M. Castilla, J. Miret, A. Camacho, J. Garcia de Vicuna, and J. Matas Alcala, "Modeling and design of voltage support control schemes for three-phase inverters operating under unbalanced grid conditions," *Power Electronics, IEEE Transactions on*, vol. PP, no. 99, pp. 1–1, 2014.
- [17] "Ieee draft recommended practice for interconnecting distributed resources with electric power systems distribution secondary networks," *IEEE P1547.6/D7.0, June 2010*, pp. 1–31, Sept 2010.
- [18] M. Marwali and A. Keyhani, "Control of distributed generation systems-part i: Voltages and currents control," *Power Electronics, IEEE Transactions on*, vol. 19, no. 6, pp. 1541–1550, Nov 2004.
- [19] R.-J. Wai, C.-Y. Lin, Y.-C. Huang, and Y.-R. Chang, "Design of high-performance stand-alone and grid-connected inverter for distributed generation applications," *Industrial Electronics, IEEE Transactions on*, vol. 60, no. 4, pp. 1542–1555, April 2013.
- [20] R. Teodorescu and F. Blaabjerg, "Flexible control of small wind turbines with grid failure detection operating in stand-alone and grid-connected mode," *Power Electronics, IEEE Transactions on*, vol. 19, no. 5, pp. 1323–1332, Sept 2004.
- [21] I. Gabe, V. Montagner, and H. Pinheiro, "Design and implementation of a robust current controller for vsi connected to the grid through an lcl filter," *Power Electronics, IEEE Transactions on*, vol. 24, no. 6, pp. 1444–1452, June 2009.
- [22] X. Wang, X. Ruan, S. Liu, and C. Tse, "Full feedforward of grid voltage for grid-connected inverter with lcl filter to suppress current distortion due to grid voltage harmonics," *Power Electronics, IEEE Transactions on*, vol. 25, no. 12, pp. 3119–3127, Dec 2010.